Process Variations and the Transient Behavior of Extruders

Rajath Mudalamane and David I. Bigio
Dept. of Mechanical Engineering, University of Maryland, College Park, MD 20742

To explain output fluctuation problems in extrusion, a transient model of material flow through an extruder is developed and used to study the transmission of external disturbances through the extruder. This model can be implemented for any extrusion geometry for which a pressure-throughput model exists. Simulation results show that every extrusion process has a characteristic critical frequency. All disturbance frequencies above this critical value are damped out and the lower frequency components are transmitted through the process with little amplitude attenuation. These low frequency disturbances are of most concern since they are not damped by the extrusion process. Extrusion screw configurations are designed to satisfy steady-state performance requirements, and nonsteady-state performance is rarely considered. The findings indicate that a two pronged approach would be required combining screw design (passive control) to handle higher frequencies and closed-loop control (active control) to detect and remove lower frequency disturbances.

Introduction

The output of an extruder almost always exhibits a complex and periodic fluctuation that is the result of the superimposed effect of external disturbances entering the process from various sources and internal flow instabilities. Under certain conditions, the amplitudes of these fluctuations are large enough to cause undesirable effects such as surging or spurt flow, bamboo fracture, sharkskin, and other forms of product nonuniformity. Die flow instability, melting instability, periodic nature of feeder screws, heating elements, nonuniform feed material quality, and the extrusion screw itself are all considered possible causes of process variations.

There are many reports of the oscillatory nature of an extruder's output in literature. Costin et al. (1982) observed the pressure at the die of a Killion 38 mm single screw extruder (SSE). They found that the pressure trace was composed of three different frequencies in accordance with Tadmor's observations (Tadmor and Gogos, 1979). By using a low-pass filter, they were able to separate the pressure trace into three distinct frequency ranges. The highest frequency disturbance was on the order of the screw speed (1.2 s at a screw speed of 50 rpm). The intermediate frequency disturbance had a period of approximately 8 s. They attributed this disturbance to solid bed instability and also observed that the frequency was unaffected by the extruder screw speed or by the type of polyethylene used. The low frequency component had a period of around 3 min.

Cyclic breakup and buildup of the solid bed in the melting section is often cited to be the most likely source of the intermediate frequency fluctuations in the SSE geometry, but it has not been proven so far. A detailed discussion of solid bed dynamics is provided by Edmondson and Fenner (1975) and Fenner et al. (1979). They measured bed width and bed velocities after rapid cooling and screw extraction. Bed velocity was inferred from striations in the frozen melt film covering the solid bed. It was found that the solid bed showed discontinuity at the same point that the bed shows acceleration. This solid bed acceleration is believed to be a source of surging behavior. However, the authors did not make the connection between solid bed acceleration and instability in the solid bed.

Costin et al. (1982) published a review of literature on modeling and control of extruders, and a substantial portion of the article discusses disturbances in extruders. Using experimentally obtained relationships between throughput and

Correspondence concerning this article should be addressed to D. I. Bigio.

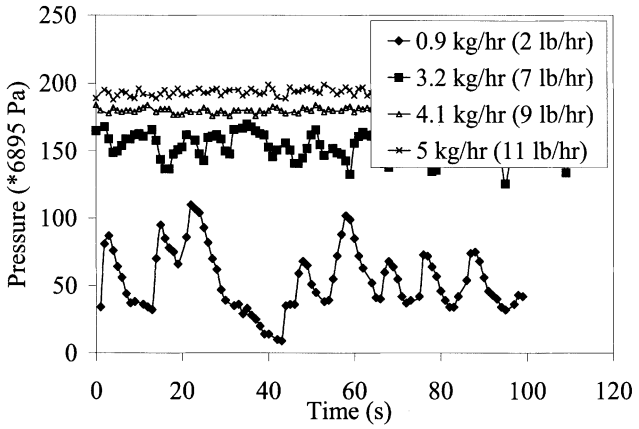

Figure 1. Pressure fluctuation (surging) as observed in a TSE at 100 rpm.

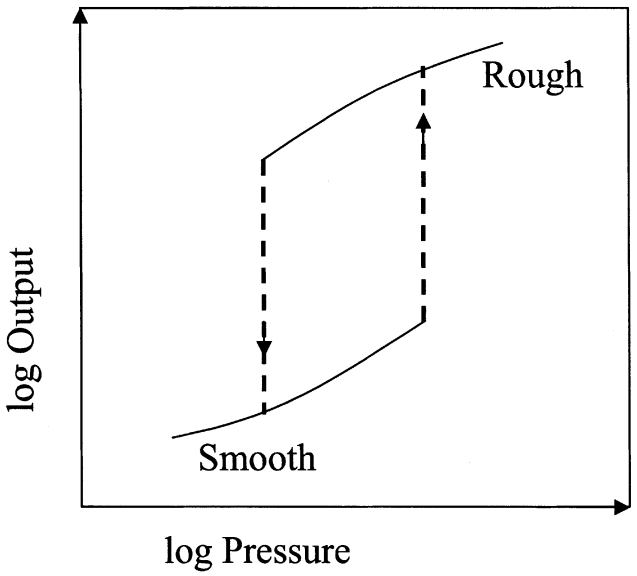

Figure 2. Typical discontinuous output-pressure curve for a linear polyethylene.

die pressure, Maddock (1964) showed that a 1% variation in pressure yields a 3% variation in throughput. He concluded that relatively small amplitude variations in pressure could result in larger variations in throughput. He also found that in extrusion of heavy wall cable, pressure surges of an amplitude of 48 kPa at an average operating level of 7.1 MPa produced a borderline product. These surges had a period of 20–30 s corresponding to intermediate frequency disturbances. He also observed high frequency surges at the same frequency as the screw speed, but these fluctuations were too rapid to appreciably change the thickness of the extrudate. Fontaine (1975), Wright (1975), and Rastogi (1978) all made observations similar to Tadmor's. However, no attempts were made to control the high and intermediate frequency disturbances. A low pass filter was often used to remove these frequencies from the signal. Costin et al. (1982) observed that a filter used to remove a noise with 11 s period would have affected a process with a 5 s time constant.

Figure 1 shows the results of an experimental study to record surging behavior in twin screw extruders (TSE) that was carried out at the Polymer Processing Laboratory, University of Maryland. The figure shows the pressure measured at the die of a 20 mm non-intermeshing TSE, under different feed rates and a constant screw speed of 100 rpm. It was found that the amplitude of the pressure fluctuations was the highest at the lowest throughput rates. At higher throughput rates (and fill levels), the pressure trace is smoother. In addition, the frequency of these fluctuations was of the same order as the screw speed of the feeder and not the screw speed of the extruder. Note that the amplitude of fluctuation at 5 kg/h (11 lb/h), is slightly higher than the amplitude at 4.1 kg/h (9 lb/h), and the frequency does not match the feed screw speed anymore. This suggests that these fluctuations could be from another source.

Many researchers have observed instabilities in the flow of certain polymeric melts through capillaries and dies. Bagley et al. (1958) reported that, with linear polyethylene, there is a pressure region where the output is double valued, that is, the log output-log pressure plot has the form shown in Figure 2 and the extruded filaments were either smooth or rough depending on the output value. According to De Kee and Wissburn (1998), there are two theories used to explain this phenomenon. The first is that this instability is due to loss of adhesion to the die wall resulting in an oscillatory stick-slip situation. The second possibility that is being explored is that the flow oscillations are the result of constitutive instability. Ramamurthy (1986) found that the assumption of no wall slip is not valid above a critical shear stress (approximately 0.1–0.14 MPa) above which surface or gross irregularities are found in both linear and branched polyethylenes. They also note that the critical shear stress is independent of the molecular structure, melt temperature, and design of the capillary. They state that breakdown of adhesion leading to the slip is the primary reason for the instability and melt fracture could be eliminated by proper choice of capillary construction material and adhesion promoters in the resin. Hatzikiriakos and Dealy (1992) proposed an empirical model to describe the pressure and flow rate oscillations in the oscillatory flow regime and found good agreement with experiments. Den Doelder et al. (1998) found that the answer to the slip or no-slip controversy is not an easy one. They studied capillary flow using three different fluid models. Two of the models—a Newtonian fluid with an alternating stick-slip boundary condition and a system of two Newtonian fluids flowing in concentric die regions with a no-slip condition—can exhibit oscillatory conditions, but not a Johnson-Segalman-Oldroyd (JSO) fluid (a nonmonotonic constitutive equation) with a no-slip condition. Fyrillas et al. (1999) found that an Oldroyd-B fluid in conjunction with a nonmonotonic slip equation can exhibit periodic oscillations.

Derezinski (1997) studied the damping effect of melt delivery systems that transport material away from the extruder to the die. It was found that, due to polymer compressibility and deformation of the system, the delivery systems can absorb some of the oscillations that exit the extruder and provide a more stable supply to the die.

Process variations could be the result of all of the above phenomena. In this article, another aspect of the extrusion

process is investigated. A model is presented of the transient behavior of an extruder based on the mechanisms by which filled regions are formed and respond to external variations. Mudalamane et al. (2003) presented a detailed study of the properties of filled regions in extruders. Twin screw extruders are usually fed at a controlled rate using feeders and are usually run at between 20–50% of their maximum capacity. The screws are partially filled and filled regions are formed where restrictive or low-pumping capacity elements are used. Hence, extruders contain sequential filled-partially filled sections. Due to this nature of extrusion processes, there is a capacitance for material in the extruder and, thus, the extrusion process will have an inherent disturbance damping ability. A transient model of the evolution of filled regions will be presented in the following section.

It should be noted that such melt flow instability is observed in the die at the end of the machine and at high throughput ranges. Hence, the effect of upstream parameters such as fill level and screw design should affect these oscillations in a different way compared to disturbances such as feed variations that pass through the extruder. Taking a second look at the data in Figure 1, it can be seen that as the throughput is increased at a given screw speed, the damping ability of the extruder improves, but at the same time at higher throughputs, there is greater risk of flow instability. As Ramamurthy (1986) showed, the presence and the nature of flow instability depends not only on the nature of the fluid, but also on the materials used in the construction of the capillary and it is largely a surface phenomenon. Due to the large number of combinations possible and due to the sensitivity of the flow to impurities or adhesion promoters that may be in the fluid, prediction of flow instability and its characteristics (frequency, amplitude, and so on) with good reliability for any given system is very difficult and has not been achieved so far. Hence, flow instability, is not included in the model presented in this article. The model of evolution of fill lengths presented here, together with the research on flow instability, provides a more complete understanding of transient phenomena in extrusion.

Theoretical Model of Transient behavior

White and Kim (2000, 2001) applied a material balance over an extruder to arrive at a differential equation that relates the flows in and out of the extruder to the change in total accumulated material in the extruder. This was then applied to the simulation of startup flow in the extruders. If, instead, the material balance is taken over each individual filled region, it allows a more general development of the model such that disturbances of arbitrary functionality and in any parameter can be tested and the effect of changing fill lengths on the delay times can be included.

Figure 3 shows a typical polymer extruder. Material is first carried into the melting section where thermoplastic components are melted before they are carried to the mixing sections. There may be more than one mixing section. Twin-screw extruders are normally starve-fed so that the filled regions are separated by partially filled zones which act mainly as transport zones. The mixing that is achieved in these regions is minimal. Another important use of the partially filled zones is that they represent the amount of room available for the filled regions to expand to accommodate changes in fill length or to respond to any disturbance.

External disturbances may enter through feed rates, feed composition, feed conditions (moisture content or temperature of the feed), heating jackets, variations in motor power, changes in environmental conditions, and so on. Such disturbances directly cause changes in fill levels, pressures, and melt temperature. In the filled regions, we have fluid enclosed within the screw channel and driven by a moving wall (barrel) and pressure within the filled region. Order of magnitude calculations based on this geometry show that the times required for the flow profiles to respond to any change in the applied pressure gradient or moving wall velocity are on the order of 10^{-6} seconds for typical polymer melts (polypropylene, polyethylene, and so on). Hence, it can be assumed that, for the time scales of interest, the flow within the filled regions is always fully developed.

Consider a partially filled–fully filled region pair (see Figure 4). The fully filled region is taken as the control volume (enclosed by dotted line in Figure 4).Taking a mass balance over the control volume, we have

$$[\text{Rate of change of accumulation in fill length}] = [\text{flow in}]\text{-}[\text{flow out}] \quad (1)$$

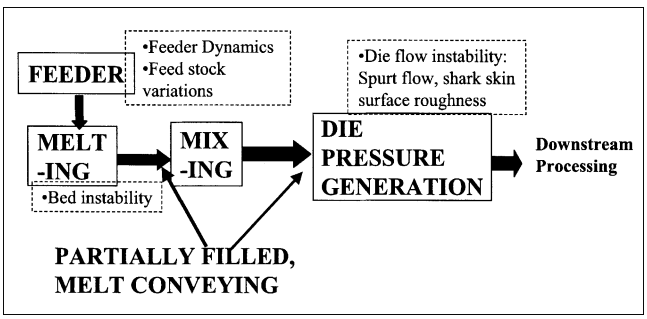

Figure 3. Polymer extruder.

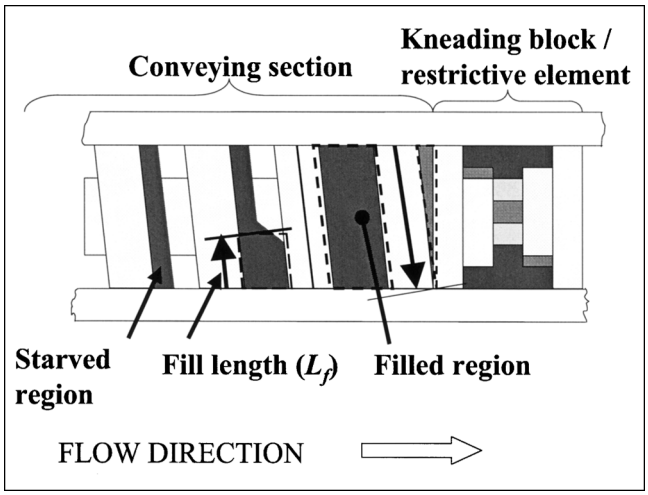

Figure 4. Filled section of an extruder.

Let Q_{in} be the total flow rate into the filled region, Q_{out} be the total flow rate out of the filled region, and Φ_f be the fill fraction at the entrance to the filled region. Any accumulation results in a change in the length L_f of the filled region. Equation 1 can be written as

$$A_c\left(1-\Phi_f\right)\frac{dL_f}{dt}=Q_{\text{in}}-Q_{\text{out}} \tag{2}$$

A_c represents the channel cross-sectional area. L_f is the length of the filled region. The screw flights and the barrel walls are assumed to be impervious to the fluid. Note that, within the filled region, any leakage flow over the flight tips ends up in the filled region as well.This is also true for conveying in the starved regions. Near the end of the fill length, there will be a short region where the clearance flow goes into the starved region. For an extruder in fair working condition, this particular leakage flow is very small compared to the overall flows and can be neglected.

Q_{in}, Q_{out} and Φ_f can all be written as functions of fill length, screw geometry, and material properties. The fractionalfill at the entrance to the fill length can be written as

$$\Phi_f(L_{st},t)=\frac{Q_{st}(L_{st},t)}{Q_{\text{drag}}}=\frac{Q_{st}\left(\left\{L-L_f\right\},t\right)}{Q_{\text{drag}}} \tag{3}$$

where Q_{st} is the flow in the starved or partially filled region and L_{st} is the length of the region. Since the flow into the extruder isn't constant, Q_{st} varies with time and position along the extruder channel. Q_{drag} is the flow capacity of the screw when there is no backpressure. Flow into the filled region is equal to the flow at the end of the starved section, that is

$$Q_{\text{in}}=Q_{st}(L_{st},t)=Q_{st}\left(\left(L-L_f\right),t\right) \tag{4}$$

In an extrusion screw operating under starved conditions, fully filled regions are formed behind sections such as kneading blocks, die, and so on, which provide resistance to flow. The helical (conveying) screw sections generate pressure to pump material through such resistances. At any time, the flow out of the filled region depends on the balance between the pumping ability of the screw and the backpressure created by the resistive elements. This implies that always

$$Q_{\text{out}}=Q_{fl}=Q_{\text{restriction}} \tag{5}$$

where Q_{fl} depends on the filled length L_f, screw speed N, the screw geometry, fluid properties, and the pressure gradient along the screw channel. This relation may be in the form of an explicit expression or a computer program. Flow through the restrictive elements also depends on the geometry, the fluid properties, and the applied pressure gradient. Specific models of flow for various types of extruder geometries are available in literature (White, 1990; Rauwendaal, 1994; Tadmor and Gogos, 1979; Meijer and Elemans, 1988; Kim and White, 1990; Jerman, 1986; Baim, 1993; Denson and Hwang, 1980; Todd et al., 2003; Szydlowski and White, 1988; Wang and White, 1989). These models relate the throughput through a section to the applied pressure gradient and this relationship can be written as

$$Q=f(dP/dz) \tag{6}$$

z is the coordinate in the downchannel direction. For a given screw geometry and fluid, there is a 1-1 relationship between throughput and pressure gradient and, hence, the inverse function f^{-1} exists. For fully developed flow, the downchannel pressure gradient is constant. If we can assume the pressure to be zero at the end of the filled section

$$P=f^{-1}(Q)*L \tag{7}$$

The pressure drop over the restriction must equal the pressure developed in the conveying sections. For example

$$\int_0^{L_f}\left[\frac{dP}{dz}\right]_{fl}dz=\int_0^{L_{\text{die}}}\left[\frac{dP}{dx}\right]_{\text{die}}dx \tag{8}$$

Also, at the point where the conveying section and restrictive section meet, the pressures have to be equal. If P_{sc} is the pressure at the exit of the filled section of forward conveying elements and $P_{\text{restriction}}$ is the pressure at the entrance of the resistive elements

$$P_{sc}=P_{\text{restriction}}\Rightarrow f_{sc}^{-1}(Q)*L_f=f_{\text{restriction}}^{-1}(Q)*L_{\text{restriction}} \tag{9}$$

Or

$$f_{sc}^{-1}(Q)*L_f-f_{\text{restriction}}^{-1}(Q)*L_{\text{restriction}}=0 \tag{10}$$

This equation can be solved to find the value of Q_{out} for a given value of L_f. Given the fill length, the screw speed, fluid properties and the geometry of the conveying and restrictive elements, the output flow rate is completely determined. In most cases, the pressure-throughput model f is not an explicit equation, but a numerical solution. The above equation then cannot be solved explicitly and a numerical procedure such as the Newton-Raphson scheme should be used to solve for Q_{out}. The exact nature of f depends on the geometry of the section under consideration. While f can be obtained for different geometries from current literature, in most cases manipulating the modeling procedure to obtain f^{-1} is not straightforward. A method for obtaining f^{-1} when f is a numerical solution is demonstrated with an example geometry in the next section. The concepts introduced in the next section can be applied to any other extrusion geometry (co-rotating intermeshing, counter rotating nonintermeshing, kneading blocks, and so on).

To summarize, Eq. 2 can be rewritten as

$$\overline{HW}\left(1-\Phi\left(L_f,t\right)\right)\frac{dL_f(t)}{dt}=Q_{st}\left(\left(L-L_f\right),t\right)-Q_{\text{out}}\left(L_f,t,\text{ geometry}\right) \tag{2b}$$

Table 1. Extruder Geometry and Fluid Properties Used in the Simulation

Screw Geometry: Single Screw, Rectangular Channel Cross Section	
Barrel I.D. (mm)	30
Screw Length	20 L/D
Initial Root Diameter (mm)	23
Pitch (mm)	30 (square pitch)
Helix angle	17.66°
Number of flight starts	1
Flight width (mm)	4
Die Geometry: Three Hole Die, Circular Cross Section	
Hole I.D. (mm)	4.2
Hole length (mm)	15.9
Fluid Properties: Power-Law Fluid	
Type	Polyethylene; Alathon (Tadmor and Gogos, 1979)
Power-Law Constant m (Pa-s)	6.79e + 3
Power-Law Index n	0.37

Q_{st} and Φ are supplied by a model of flow in the starved or partially filled regions. Q_{out} is calculated by combining the pressure-throughput relationships for the conveying section and the restrictive elements.

Model Implementation for an Example Geometry

The model was implemented for a single screw section of length 20 L/D that pumps material through a 3-hole die. The geometry is described in Table 1. Figure 5 explains the geometric constants for the screw. The channels are rectangular in the cross section. It is assumed that the extruder is fed with polymer melt and there is no phase change within the extruder. Since the aspect ratio of the channel is small, the effect of the side walls is neglected. Isothermal conditions are assumed. Effects of curvature are neglected and the screw channel is unwound from the root to form a flat rectangular channel, as shown in Figure 6. As it was explained in the previous section, due to the high viscosity of polymer melts, the response of flow fields to changes at the boundaries is very fast compared to the transient response speed of the extruder. Hence, the flow is considered to be fully developed at all times. Now, the cross channel and downchannel components of the velocity vector are functions of depth only, that is, $v_x = v_x(y)$ and $v_z = v_z(y)$. The equations of motion then reduce to

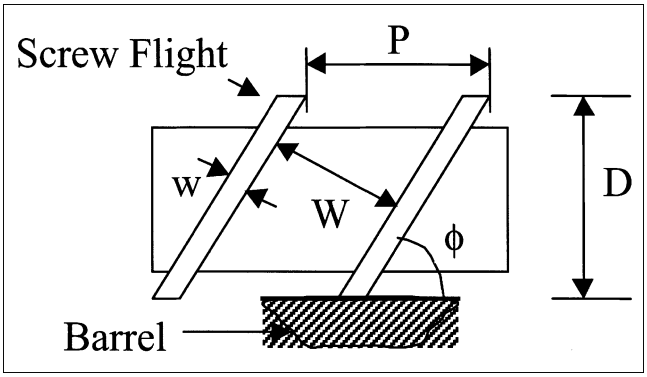

Figure 5. Description of screw geometry constants.

$$-\frac{\partial \tau_{yx}}{\partial y} = \frac{\partial P}{\partial x} \Rightarrow -\tau_{yx} = \frac{\partial P}{\partial x} y + C_1 \tag{11}$$

$$-\frac{\partial \tau_{yz}}{\partial y} = \frac{\partial P}{\partial z} \Rightarrow -\tau_{yz} + \frac{\partial P}{\partial z} y + C_2 \tag{12}$$

C_1 and C_2 are constants of integration. The fluid is assumed to be shear thinning. Applying the Ostwald-De Waele model (Bird et al., 1977)

$$\tau = -m[\Delta:\Delta]^{(n-1)/2}\Delta \tag{13}$$

where τ is the stress tensor and Δ is the rate of deformation tensor and $\Delta:\Delta$ is the second invariant. Therefore

$$\tau_{yx} = -m\left[\sqrt{\left(\frac{dv_x}{dy}\right)^2 + \left(\frac{dv_z}{dy}\right)^2}\right]^{n-1}\frac{dv_x}{dy} \tag{14}$$

$$\tau_{yz} = -m\left[\sqrt{\left(\frac{dv_x}{dy}\right)^2 + \left(\frac{dv_z}{dy}\right)^2}\right]^{n-1}\frac{dv_z}{dy} \tag{15}$$

Substituting Eqs. 14 and 15 into Eqs. 11 and 12 and rearranging, we get

$$\frac{dv_x}{dy} = \frac{\left(\frac{\partial P}{\partial x} y + C_1\right)}{m^{1/n}}\left[\left(\frac{\partial P}{\partial x} y + C_1\right)^2 + \left(\frac{\partial P}{\partial z} y + C_2\right)^2\right]^{\frac{1-n}{2n}} \tag{16}$$

$$\frac{dv_z}{dy} = \frac{\left(\frac{\partial P}{\partial z} y + C_2\right)}{m^{1/n}}\left[\left(\frac{\partial P}{\partial x} y + C_1\right)^2 + \left(\frac{\partial P}{\partial z} y + C_2\right)^2\right]^{\frac{1-n}{2n}} \tag{17}$$

where C_1 and C_2 are constants of integration. The boundary conditions are

$$y = 0\begin{cases} v_x = 0 \\ v_z = 0 \end{cases} \tag{18}$$

$$y = H\begin{cases} v_x = v_{Bx} \\ v_z = v_{Bz} \end{cases} \tag{19}$$

Since there is no net flow in the cross-channel direction and the net flow in down-channel direction is the throughput Q, we can write

$$W * \int_0^H v_x dy = 0 \tag{20}$$

$$W * \int_0^H v_x dy = Q \tag{21}$$

C_1, C_2, $\partial P/\partial x$, and $\partial P/\partial z$ are unknown in Eqs. 16 and 17. Equations 16 and 17 need to be integrated with condition 18 and so that the conditions 19–21 are met. Define residuals as

$$R_{Vx} = \int_0^H \frac{\partial v_x}{\partial y} dy - v_{bx} \tag{22}$$

$$R_{Vz} = \int_0^H \frac{\partial v_z}{\partial y} dy - v_{bz} \tag{23}$$

$$R_{Qx} = \int_0^H v_x dy - 0 \tag{24}$$

$$R_{Qz} = W * \int_0^H v_z dy - Q \tag{25}$$

These residuals are functions of C_1, C_2, $\partial P/\partial x$ and $\partial P/\partial z$. The Newton-Raphson scheme for multiple variables is used to solve for C_1, C_2, $\partial P/\partial x$ and $\partial P/\partial z$ so that the residuals go to zero. Initial values are calculated using expressions obtained from the solution of the same problem for a Newtonian fluid. Applying the Newton-Raphson method to this problem, we get

$$\begin{bmatrix} R_{vx} \\ R_{vz} \\ R_{Qx} \\ R_{Qz} \end{bmatrix}_k = \begin{bmatrix} \frac{\partial R_{vx}}{\partial C_1} & \frac{\partial R_{vx}}{\partial C_2} & \frac{\partial R_{vx}}{\partial(\partial P/\partial x)} & \frac{\partial R_{vx}}{\partial(\partial P/\partial z)} \\ \frac{\partial R_{vz}}{\partial C_1} & \frac{\partial R_{vz}}{\partial C_2} & \frac{\partial R_{vz}}{\partial(\partial P/\partial x)} & \frac{\partial R_{vz}}{\partial(\partial P/\partial z)} \\ \frac{\partial R_{Qx}}{\partial C_1} & \frac{\partial R_{Qx}}{\partial C_2} & \frac{\partial R_{Qx}}{\partial(\partial P/\partial x)} & \frac{\partial R_{Qx}}{\partial(\partial P/\partial z)} \\ \frac{\partial R_{Qz}}{\partial C_1} & \frac{\partial R_{Qz}}{\partial C_2} & \frac{\partial R_{Qz}}{\partial(\partial P/\partial x)} & \frac{\partial R_{Qz}}{\partial(\partial P/\partial z)} \end{bmatrix}_k * \begin{bmatrix} \Delta C_1 \\ \Delta C_2 \\ \nabla(\partial P/\partial x) \\ \Delta(\partial P/\partial z) \end{bmatrix}_k \tag{26}$$

$$\begin{bmatrix} C_1 \\ C_2 \\ (\partial P/\partial x) \\ (\partial P/\partial x) \end{bmatrix}_{k+1} = \begin{bmatrix} C_1 \\ C_2 \\ (\partial P/\partial x) \\ (\partial P/\partial x) \end{bmatrix}_k + \left\{ \begin{bmatrix} \frac{\partial R_{vx}}{\partial C_1} & \frac{\partial R_{vx}}{\partial C_2} & \frac{\partial R_{vx}}{\partial(\partial P/\partial x)} & \frac{\partial R_{vx}}{\partial(\partial P/\partial z)} \\ \frac{\partial R_{vz}}{\partial C_1} & \frac{\partial R_{vz}}{\partial C_2} & \frac{\partial R_{vz}}{\partial(\partial P/\partial x)} & \frac{\partial R_{vz}}{\partial(\partial P/\partial z)} \\ \frac{\partial R_{Qx}}{\partial C_1} & \frac{\partial R_{Qx}}{\partial C_2} & \frac{\partial R_{Qx}}{\partial(\partial P/\partial x)} & \frac{\partial R_{Qx}}{\partial(\partial P/\partial z)} \\ \frac{\partial R_{Qz}}{\partial C_1} & \frac{\partial R_{Qz}}{\partial C_2} & \frac{\partial R_{Qz}}{\partial(\partial P/\partial x)} & \frac{\partial R_{qz}}{\partial(\partial P/\partial z)} \end{bmatrix}^{-1} * \begin{bmatrix} R_{vx} \\ R_{vz} \\ R_{Qx} \\ R_{Qz} \end{bmatrix} \right\} \tag{27}$$

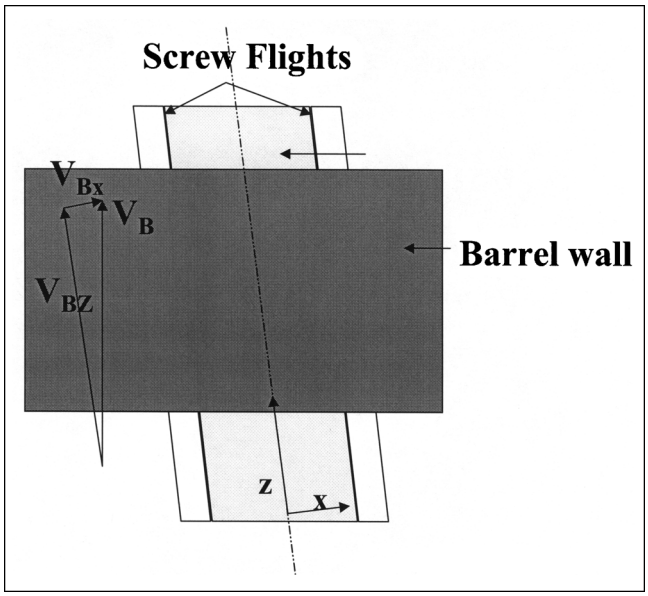

Figure 6. Unwound screw forms a rectangular channel with the barrel wall moving at an angle ϕ to the axis.

where k is the iteration number. The residuals at each point k are obtained by integrating Eqs. 16 and 17 using the initial values from Eq. 18 and the current values of C_1, C_2, $\partial P/\partial x$ and $\partial P/\partial z$. The partial derivatives are obtained by re-evaluating the residuals after perturbing each of the parameters C_1, C_2, $\partial P/\partial x$ and $\partial P/\partial z$, by a small amount. Equation 27 converges quickly and yields sufficiently low residual values in less than 10 iterations.

Note that the above numerical solution yields $\partial P/\partial z$ for a given value of throughput Q. Hence, this solution is in fact the f^{-1} of Eq. 7 and the f_{sc}^{-1} of Eq. 10. The dimensionless

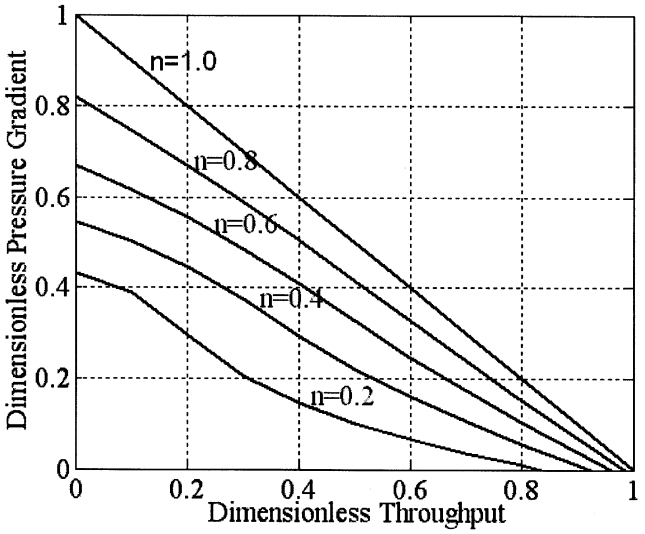

Figure 7. The inverse pressure-throughput relationship plot (f_{sc}^{-1}).

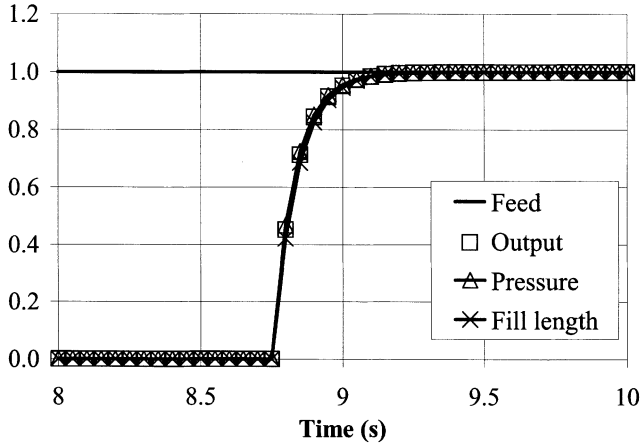

Figure 8. Response to step change in input flow rate from 22.7 to 27.27 kg/h (50–60 lb/h) at 300 rpm: the step was given at time $t = 0$.

pressure gradient and dimensionless throughput can be defined as (Rauwendaal, 1994)

$$\left(\frac{dP}{dz}\right)^{o} = \frac{\left(\frac{dP}{dz}\right)}{\left[\frac{6m}{H}\left(\frac{v_{Bz}}{H}\right)^{n}\right]} \tag{28}$$

and

$$Q^{o} = \frac{2Q}{WHv_{Bz}} \tag{29}$$

The inverse model can be validated by generating curves of a dimensionless pressure gradient as a function of the throughput at different values of the power law index n and plotting them, as shown in Figure 7. If this figure is flipped so that the pressure gradient is the x-axis, the curves line up exactly with dimensionless throughput vs. pressure gradient curves generated for the same geometry by Rauwendaal (1994).

The isothermal pressure flow of a Power law fluid through the die hole of diameter D_{die} and length L_{die} can be written as (Rauwendaal, 1994)

$$\frac{Q_{\text{die}}}{\text{Per hole}} = \left(\frac{\pi D_{\text{die}}^3}{8(s+3)}\right)\left(\frac{D_{\text{die}}}{4m}\frac{\Delta P_{\text{die}}}{L_{\text{die}}}\right)^{1/n} \tag{30}$$

Hence

$$\Delta P_{\text{die}} = L_{\text{die}} * f_{\text{die}}^{-1}(Q)$$

$$= L_{\text{die}} * \left\{\frac{4m}{D_{\text{die}}}\left[\left(\frac{Q_{\text{die}}}{\text{Per hole}}\right)\frac{8(s+3)}{\pi D_{\text{die}}^3}\right]^{n}\right\} \tag{31}$$

Equation 10 is solved together with Eqs. 27 and 31 to calculate Q_{out} for Eq. 2 at a given value of fill length L_f. Hence, the solution of Eq. 10 involves a Newton-Raphson scheme nested within another Newton-Raphson scheme in this case.

Booy (1980) showed that the average velocity of the material being transported in a partially filled section could be written as

$$\overline{U} = \frac{v_{bz}}{2} = \frac{\pi DN\cos\theta}{2} \tag{32}$$

where v_{Bz} is the downchannel component of the barrel velocity, D is the Barrel I.D., and ϕ is the helix angle of the screw. Assuming pure plug flow in the starved regions (no axial mixing), if $Q_{\text{feed}}(t)$ is the feed into the starved section, then the flow rate in the section at any time and any location L_{st}, can be written as

$$Q_{st}(L_{st},t) = Q_{\text{feed}}(t - t_d) = Q_{\text{feed}}\left(t - \frac{L_{st}}{\overline{U}}\right) \tag{33}$$

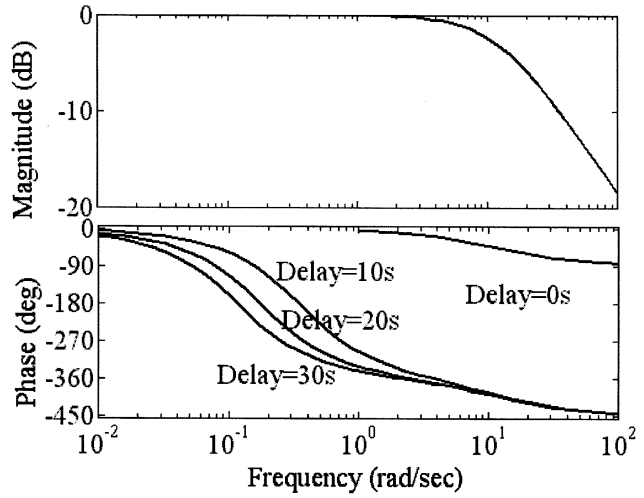

Figure 9. Frequency response of the system.

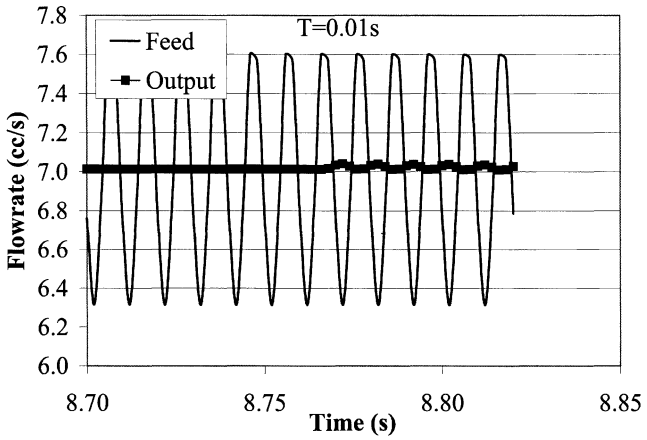

Figure 10. Response to a sinusoidal input of time period $T = 0.01$ s and amplitude 2.27 kg/h.

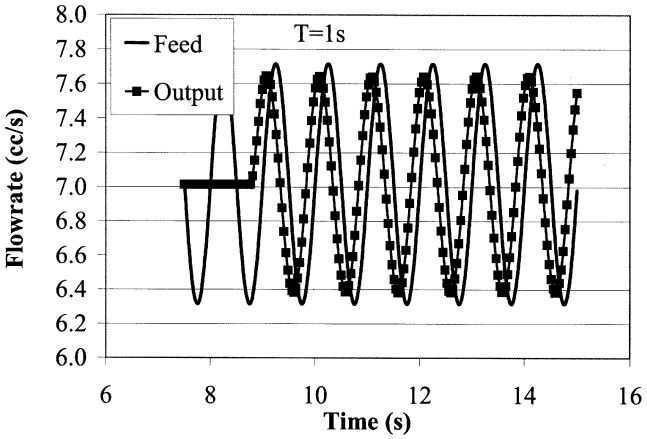

Figure 11. Response to a sinusoidal input of period 1s shows little damping.

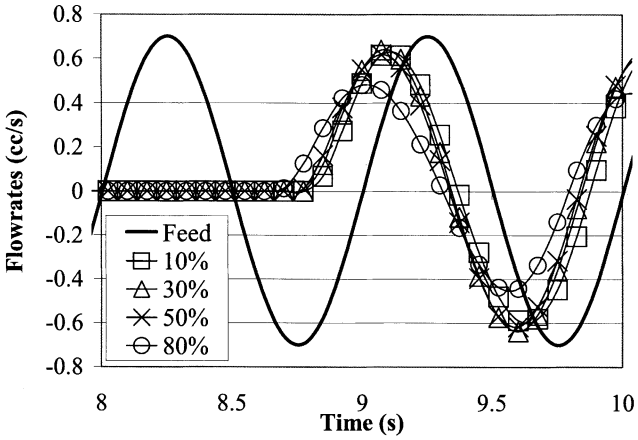

Figure 13. Effect of percent fill on response to a sinusoidal input in feed rate.

Using Eq. 34, t_d can be written as

$$t_d = \frac{2(L - L_f)}{\pi DN \cos \phi} \tag{34}$$

All the variables on the righthand side of Eq. 2b have now been expressed as functions of fill length and time. A 4th-order Runge-Kutta procedure was used to solve Eq. 2b. The algorithm was implemented in MATLAB. Note that the models used in this section assumed isothermal conditions. If temperature effects and disturbances entering through heating elements are of concern, nonisothermal models of flow should be employed. The development of the transient model would still follow the same steps outlined above.

Step Response of the Extruder and Inherent Damping Characteristics

Figure 8 shows the response of output flow rate to a step change in input flow rate from 22.7 to 27.7 kg/hr (50 to 60 lb/h) for a screw of depth 3.6 mm (0.14 in.). A transfer function model (with one pole) was identified with the step response in order to study the frequency response of the system (Figure 9). It can be seen that after $w = 10$ rad/s, the signal amplitude starts to drop very rapidly. This corresponds to a period of 0.628 s. It was found that changing the length of the extruder under the same conditions affects only the delay time. Hence, it had no effect on this critical frequency. However, the dead time does affect the phase of the output. The responses of the system to sinusoidal inputs of a period lower and higher than this critical level are shown in Figures 10 and 11. Disturbances of frequency higher than this critical frequency are damped effectively. It is the low frequency disturbances that are of concern because the extruder is incapable of absorbing them. However, such disturbances should be easier to measure and control by feedback methods. This suggests a two-pronged approach with active feedback control for low-frequency disturbance rejection and robust process design to reject intermediate to high frequency disturbances (passive control) to cover the frequency band of expected disturbances.

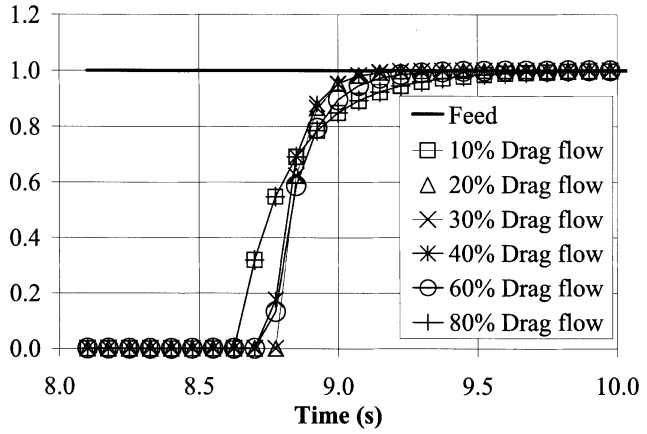

Figure 12. Effect of percent fill on step response of extruder.

Effect of Operating Conditions on Damping Ability

Figure 12 shows the response of output flow rate to steps of size 2.27 kg/hr (5 lb/h), given at different fill levels. Percent drag flow is defined as the ratio of feed flow rate to the maximum flow rate capacity of the screw. It was observed that the response is more damped at higher percent drag flows. Figure 13 shows the response to a sinusoidal input flow rate of the same amplitude and frequency under different conditions of fill. Again, the screw shows better damping at the higher percent drag flow. It can be seen from Eq. 5 that for higher percent fill Φ, the rate of change of L_f is higher for the same size step input of flow rate. However, the change of ΔL_f is greater for the same step. The time to reach steady state is the result of these two opposing effects. At higher fill levels, the latter effect dominates since there is very little empty channel space left. Given the same conditions of fill and magnitude of the step input, a deeper screw (higher channel cross-sectional area) has a lower rate of change of L_f throughout. However, the change of ΔL_f is smaller. These opposing tendencies influence the time to reach steady state.

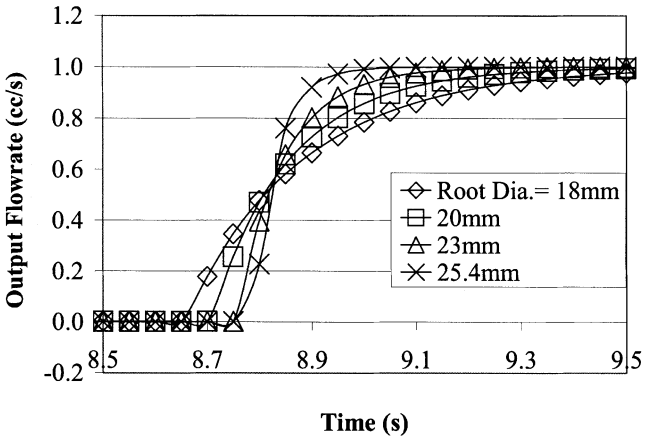

Figure 14. Effect of screw depth on step response.

Effect of Screw Depth on Transient Response

See Figures 14 and 15. In all cases, the step changes in feed rate were given at 50% drag flow to obtain same fill conditions. The size of the step was 2.27 kg/h (5 lb/h) in all cases. It was found that the deepest screw exhibits the most damped response.

Perturbations in screw speed

Figure 16 shows the response of system parameters to a step change in the screw speed from 300 to 250 rpm with all other parameters including the throughput held constant. The output flow rate drops initially and then settles back to the original level by 0.2 s. This self-leveling response is observed since the output rate has to equal the input rate to the extruder. Since the pressure is determined by the throughput, it too has a similar self-leveling response. The fill length changes to a new steady-state value because the different screw speed changes the flow fields and, hence, the pressure gradient in the filled region. This change in fill length is the cause for the brief transient period. The obvious question that follows would be that, since a change in screw speed doesn't result in a change in throughput and pressure after the transient period, could they be controlled using screw speed at all?

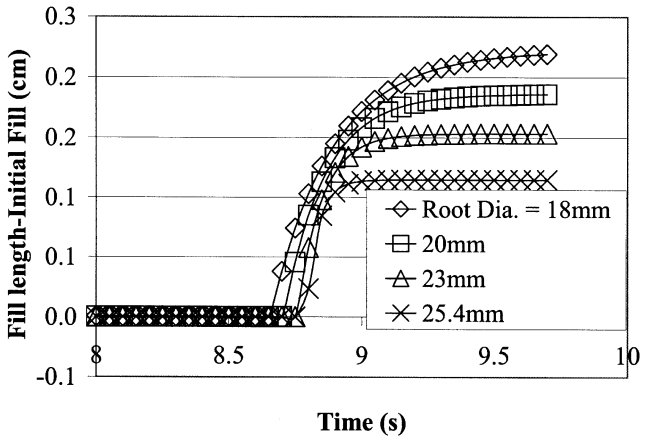

Figure 15. Step response of fill length at different depths.

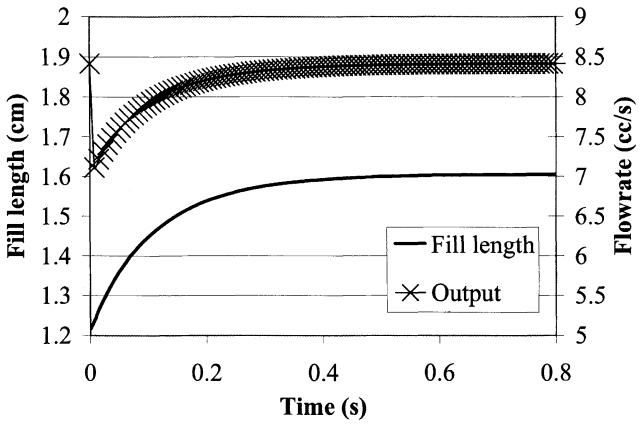

Figure 16. In response to a step input in screw speed (N) given at $t = 0$, the throughput returns to its original value (self-leveling behavior) and the fill length goes to a new final value.

The response of the system to sinusoidal disturbances in screw speed of magnitude 5 rpm with a mean level of 300 rpm (this corresponds to 3.33%) and of different frequencies is shown in Figure 17. The amplitude of the output flow rate was 1.5% at $T = 1$ s. It drops to 0.16% at $T = 10$ s. In other words, to control low frequency disturbances with $T \sim 10$ s in the output flow rate, the magnitude of the changes in screw speed required would be around 20 times the amplitude of the disturbance. Hence, the effect of screw speed on the output decreases with decreasing frequency of the input. Screw speed has the advantage of having an immediate effect on the output, but this effect is brief and, hence, this parameter is effective as a control variable for higher frequency variations, and, below a certain frequency, the output is too insensitive to changes in screw speed. The exact range of fre-

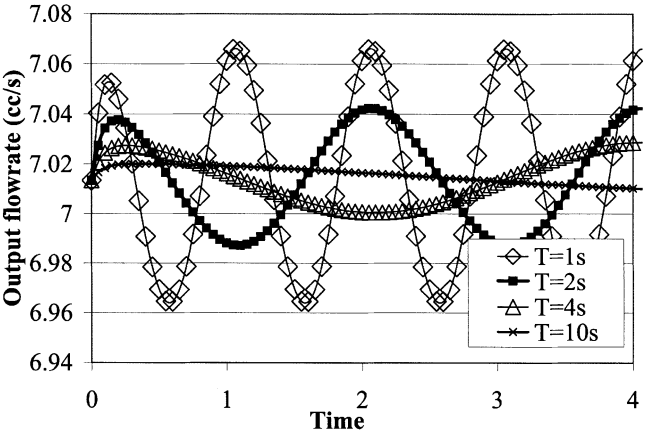

Figure 17. Output response to sinusoidal inputs in screw speed of different time periods and constant amplitude (5 rpm at a mean level of 300 rpm).

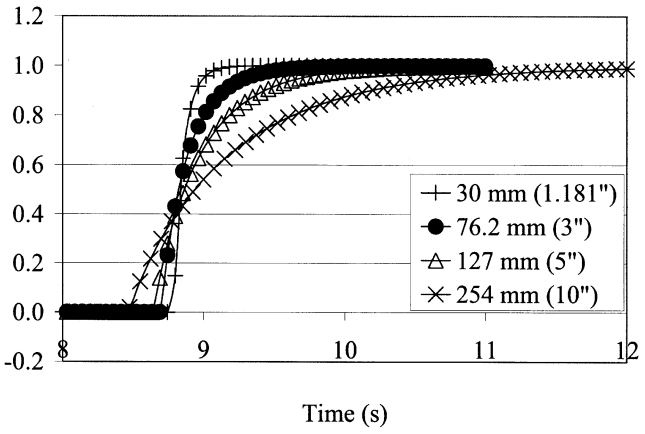

Figure 18. Response of machines of various sizes to a step change in feed flow rate.

quencies for which the screw speed is effective depends on the screw design and can be evaluated by implementing the transient model for the screw design under study.

Machine Size or Scaling

Figures 18 and 19 show the effect of machine size. It was seen that larger machines of equivalent geometry have better disturbance damping capability when compared to the smaller machines. The aspect ratio, that is, the ratio of screw depth to channel width, was kept constant for all sizes. The die opening was also increased in proportion to the machine size.

Concluding Comments

The tools presented in this article will allow designers to incorporate transient behavior into the screw design process so that frequencies of concern are damped out by the inherent disturbance damping ability of the extrusion process. A model of the transient response of an extruder based on the mechanisms by which filled regions are formed and respond to external disturbances was developed and demonstrated for a single screw extruder with a 3-hole die that is processing polyethylene (shear thinning fluid). The model can be applied to any other extrusion geometry and fluid, if pressure-throughput relationships are available. A method by which solutions of flow in an extrusion geometry can be modified to yield throughput-pressure relationships (inverse P-Q relations) was developed and demonstrated for the case under study. Simulation studies on one partially filled–fully filled region revealed that a given screw design has a characteristic critical frequency above which disturbances are damped effectively. However, disturbances of lower frequency reach the output with little damping.

An important observation is that the response is stable over the entire frequency range contrary to the observations of Levine et al. (1987). Costin et al. (1982) found that the performance of a self-tuning regulator (STR) attempting to reject surging disturbances at the output of an extruder was severely hampered by the wide range of frequencies that are superimposed in the pressure signal. The STR would tune itself to handle one frequency range, resulting in poorer performance at other ranges. With a PID algorithm, the controller tuned for good performance in one frequency range would be ineffective at rejecting other frequencies. Hence, a combination of screw design to damp out higher frequencies and closed loop-control to handle the low frequency range is required to effectively handle output fluctuations.

A study of current literature on instability in polymer flows shows that the presence and the nature of flow instability depends not only on the nature of the fluid, but also on the materials used in the construction of the capillary and is largely a surface phenomenon and there are no reliable methods of predicting these variations. However, if the frequency range of the resulting variations is known for the system under study, closed-loop control can be used to remove these low frequency range disturbances.

The response of output flow rate and die pressure is similar to that of a self-leveling system—these parameters return to their original levels after an initial transient period. However, the screw speed can be used to control output flow rates provided that the time period of the input variations are shorter than the transient period mentioned above.

Further, for a given screw design, the response is more sluggish (better damping) at higher percent fills. Deeper screws exhibit better damping ability. The relationship between fill lengths and operating conditions at steady state is nonlinear and the shape of this curve depends on the geometry under study (Mudalamane et al., 2003). The model needs to be implemented for the screw design under study. The resulting simulations can be used to guide the design to handle transients of concern.

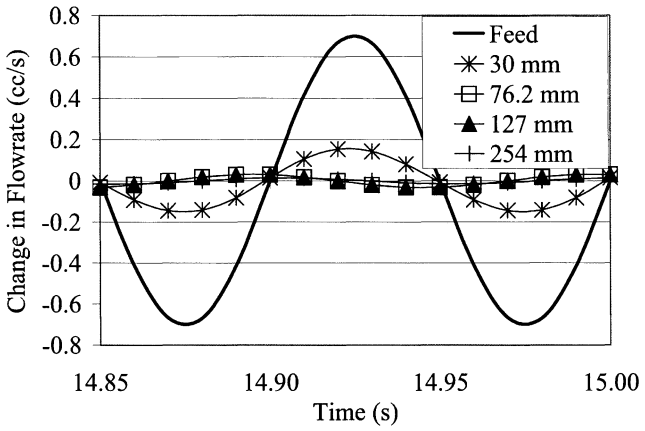

Figure 19. Effect of machine size on response to a sinusoidal input in feed rate of constant time period ($T = 0.1$ s) and amplitude (2.27 kg/h).

Notation

A_c = cross-sectional area of screw channel
Δ = rate of deformation tensor
$\Delta:\Delta$ = second invariant (scalar) of the rate of deformation tensor
Φ_f = fill level at the end of the filled region
H = channel depth
L = total length of the filled–partially filled section
L_f = length of filled region
m = power law constant

n = power law index
Q_{drag} = open discharge flow rate for the section
Q_{fl} = flow in the filled region
Q_{in} = flow into the control volume
Q_{out} = flow out of the control volume
Q_{st} = throughput in the starved or partially filled region
τ = stress tensor
v_z = downchannel component of velocity
v_x = crosschannel component of velocity
v_{Bz} = downchannel component of barrel velocity
v_{Bx} = crosschannel component of barrel velocity
V_f = volume in filled region or control volume
W = channel width

Literature Cited

Bagley, E. B., I. M. Cabott, and D. C. West, "Discontinuity in the Flow Curve of Polyethylene," *J. Appl. Phys.*, **29**(1), 109 (1958).

Baim, W., "Summary of Drag Flow Calculations for NITSE and the CoTSE," Masters Thesis, University of Maryland (1993).

Bird, R. B., R. C. Armstrong, and O. Hassager, *Dynamics of Polymeric Liquids: Volume I, Fluid Mechanics*, Wiley, New York (1977).

Booy, M. L., "Isothermal Flow of Viscous Liquids in Corotating Twin Screw Devices," *Poly. Eng. & Sci.*, **20**, 1223 (1980).

Costin, M. H., P. A. Taylor, and J. D. Wright, "On the Dynamics and Control of a Plasticating Extruder," *Poly. Eng. Sci.*, **22**(17), 1095 (1982).

Costin, M. H., P. A. Taylor, and J. D. Wright, "A Critical Review of Dynamic Modeling and Control of Plasticating Extruders," *Poly. Eng. &, Sci.*, **22**(7), 393 (1982).

De Kee, D., and K. F. Wissburn, "Polymer Rheology," *Physics Today*, **51**, 24 (June 1998).

Den Doelder, C. F. J., R. J. Koopmans, J. Molenaar, and A. A. F. Van de Ven, "Comparing the Wall Slip and the Constitutive Approach for Modeling Spurt Instabilities in Polymer Melt Flows," *J. Non-Newtonian Fluid Mech.*, **75**, 25 (1998).

Denson, C. D., and B. K. Hwang, "The Influence of Axial Pressure Gradient on Flow Rate for Newtonian Liquids in a Self Wiping, Co-Rotating Twin Screw Extruder," *Poly. Eng. Sci.*, **20**(14), 965 (1980).

Derezinski, S. J., "Calculating Surge Dampening in Melt Delivery Systems," *Society of Plastics Engineers Ann. Tech. Conf.*, Toronto, SPE, CT (May 1997).

Edmondson, I. R., and R. T. Fenner, "Melting of Thermoplastics in Single Screw Extruders," *Polymer*, **16**, (1975).

Fenner, R. T., A. P. D. Cox, and D. P. Isherwood, "Surging in Screw Extruders," *Polymer*, **20**, 733 (1979).

Fontaine, W., "Analysis and Modeling of the Dynamic Behavior of Extruders," PhD Diss., Ohio State University (1975).

Fyrillas, M., G. Georgiou, D. Vlassopoulos, and S. G. Hatzikiriakos, "A Mechanism for Extrusion Instabilities in Polymer Melts," *Poly. Eng. & Sci.*, **39**(12), 2498 (1999).

Hatzikiriakos, S. G., and J. M. Dealy, "Role of Slip and Fracture in the Oscillating Flow of HDPE in a Capillary," *J. Rheology*, **36**, 845 (1992).

Jerman, R. E., "A Mathematical Model for Non-Newtonian Melt Flow over Cylindrical Compounders in Non-Intermeshing Twin Screw Extruders," *SPE Ann. Tech. Conf.*, Boston, **32**, (1986).

Kim, M. H., and J. L. White, "A Non-Newtonian Model of Flow in Forward and Backward Pumping Screw Regions of a Modular Tangential Counter-Rotating Twin-Screw Extruder," *J. Non-Newtonian Fluid Mech.*, **37**, 37 (1990).

Levine, L., S. Symes, and J. Weimer, "A Simulation of the Effect of Formula and Feed Rate Variations on the Transient Behavior of Starved Extrusion Screws," *Biotechnol. Prog.*, **3**(4), 221 (1987).

Maddock, B. H., "Effect of Wear on the Delivery Capacity of Extruder Screws," *S.P.E.J.*, **20**, (1964).

Meijer, H. E. H., and P. H. M. Elemans, "The Modeling of Continuous Mixers. Part I: The Corotating Twin-Screw Extruder," *Poly. Eng. & Sci.*, **28**(5), 275 (1988).

Mudalamane, R., D. I. Bigio, D. C. Tomayko, and M. Meissel, "Behavior of Fully Filled Regions in an Non-Intermeshing Twin Screw Extruder," *Poly. Eng. & Sci.*, in press (2003).

Ramamurthy, A. V., "Wall Slip in Viscous Fluids and Influence of Materials of Construction," *J. Rheology*, **30**, 337 (1986).

Rastogi, L. K., "A Flat Die Extrusion Control System using Distributed Microcomputers," *Proc. Joint Auto. Control Conf.*, 375 (1978).

Rauwendaal, C., *Polymer Extrusion*, Hanser, New York (1994).

Szydlowski, W., and J. L. White, "A Non-Newtonian Model of Flow in a Kneading Disc Region of a Modular Intermeshing Corotating Twin Screw Extruder," *J. Non-Newtonian Fluid Mech.*, **28**, 29 (1988).

Tadmor, Z., and C. Gogos, *Principles of Polymer Processing*, Wiley, New York (1979).

Tadmor, Z., and I. Klein, *Engineering Principles of Plasticating Extrusion*, Van Nostrand Reinhold, New York (1976).

Todd, D. B., A. M. Robbe, and L. P. B. M. Janssen, "Flow Behavior of Newtonian Fluid through Conveying Elements and Kneading Blocks," *SPE Ann. Tech. Conf.*, Nashville, **49**, (2003).

Wang, Y., and J. L. White, "Non-Newtonian Flow Modeling in the Screw Regions of an Intermeshing Corotating Twin Screw Extruder," *J. Non-Newtonian Fluid Mech.*, **32**, 19 (1989).

White, J. L., and E. K. Kim, "Superposed Hydrodynamic Disturbances From Feeders in a Starved Flow Modular Intermeshing Co-Rotating Twin Screw Extruder," *Poly. Eng. & Sci.*, **41**(2), 233 (2001).

White, J. L., and E. K. Kim, "Transient Start-up Flow in a Modular Co-Rotating Twin Screw Extruder," *SPE Ann. Tech. Conf.*, Orlando, FL, **46** (2000).

White, J. L., *Twin Screw Extrusion*, Hanser, New York (1990).

Wright, J. O., "An Investigation of Extrusion Control Strategies by Digital Solution of Dynamic Extrusion Model," PhD Diss., Ohio State University (1975).

Manuscript received Jan. 11, 2003, and revision received May 12, 2003.